



Detection of quasi-periodic oscillations from the blazar PKS 1510-089

XIAO-PAN LI^{1,*} , LUN ZHAO¹, YUE YAN¹, LI-SHA WANG¹, HAI-TAO YANG¹, YAN CAI¹ and YU-HUI LUO^{1,2}

¹College of Physics and Information Engineering, Zhaotong University, Zhaotong 657000, China.

²Faculty of Civil Engineering and Mechanics/Faculty of Science, Kunming University of Science and Technology, Kunming 650500, China.

*Corresponding author. E-mail: lxpzrc@163.com

MS received 24 February 2021; accepted 10 May 2021

Abstract. We report the detection of quasi-periodic oscillations (QPOs) in the radio light curve of the blazar PKS 1510-089 spanning nearly 38 years, by means of the weighted wavelet Z-transform and Lomb–Scargle periodogram methods. Prominent QPOs with high confidence ($>4\sigma$) of 570 ± 30 , 800 ± 30 , and 1070 ± 40 days in the 8 GHz light curve, 430 ± 10 and 1080 ± 30 days in the 14.5 GHz light curve have been identified after estimating the significance against the red noise background. Moreover, the most significant QPO of about 1080 days exceeded 4σ confidence level at two of the three frequencies but did not exactly persist the whole observations, indicating that QPOs in blazars are transient in nature. We suggest that the search for QPO in blazar light curves should evaluate the statistical significances and consider the influences of the colored noise, after reviewing earlier QPO claims of PKS 1510-089.

Keywords. BL Lacertae objects: general—BL Lacertae objects: individual: PKS 1510-089—method: time-series analysis.

1. Introduction

Blazars are the most active subclass of radio-loud active galactic nuclei, which show luminous and violent variability in all spectral bands. Flux variability of blazars has been detected on all accessible time scales ranging from minutes through days to years. Although the variability is stochastic and aperiodic in nature, there have been quasi-periodic oscillation (QPO) claims with high statistical significance reported in recent years (King *et al.* 2013; Ackermann *et al.* 2015; Graham *et al.* 2015; Mohan *et al.* 2016; Sandrinelli *et al.* 2016a,b; Li *et al.* 2017; Gupta *et al.* 2018, 2019; Zhang *et al.* 2018; Zhou *et al.* 2018; Bhatta 2019; Kushwaha *et al.* 2020; Sarkar *et al.* 2020 and references therein). In particular, on long-term timescales, QPO claims at radio frequencies have been accumulated in several blazars: PKS 1510-089 (Xie *et al.* 2008), J1359 + 4011 (King *et al.* 2013), NRAO 530 (An *et al.* 2013), PKS 1156 + 295 (Liu & Liu 2014; Wang *et al.* 2014), PKS 0219-164 (Bhatta 2017), S5

0716 + 714 (Li *et al.* 2018), J1043 + 2408 (Bhatta 2018), AO 0235 + 164 (Raiteri *et al.* 2001; Tripathi *et al.* 2021). Since the QPO is obviously associated with the blazar phenomenologies, search and interpretation for QPO play an important role in understanding the emission processes of blazars.

The blazar PKS 1510-089 ($z = 0.036$; Thompson *et al.* 1990) is one of the brightest and most variable extragalactic sources and classified as a flat spectrum radio quasar (a subclass of blazar). This source is an extensively monitored and studied blazar that exhibits a very interesting activity at all wavelengths from radio to γ -rays, a core-dominated radio structure, very high energy emission, high polarization degree, rapid variations of polarization, and simultaneous radio and γ -ray flares. Over the past few decades, a number of ground and space monitoring programs, such as International Gamma-Ray Astrophysics Laboratory, *Fermi*-LAT, *Swift*, Small and Moderate Aperture Research Telescope System, Owens Valley Radio Observatory, and University of Michigan Radio Astronomical Observatory

Table 1. Observational log of the UMRAO monitoring.

Frequency (GHz)	Number	Time span	Duration (year)	Flux range (Jy)	Average flux (Jy)	F_{var} (%)
4.8	698	1979.03–2012.04	33.2	0.16–5.00	2.25 ± 0.08	31.30 ± 0.85
8	1235	1974.09–2012.05	37.7	0.67–6.57	2.49 ± 0.07	35.17 ± 0.71
14.5	1491	1974.08–2012.05	37.8	0.93–6.60	2.40 ± 0.06	41.11 ± 0.76

(UMRAO), have been regularly or irregularly performed to observe PKS 1510-089, which provide a mass of data set for studying the phenomenologies, multiwavelength activities, and theoretical models of this source. For characteristics and monitoring programs mentioned above, and recent multiwavelength studies refer to Aleksić *et al.* (2014), Castignani *et al.* (2017), Ahnen *et al.* (2017), Beaklini *et al.* (2017), Park *et al.* (2019), and references therein. Furthermore, there is evidence for the year-like periodicity of PKS 1510-089 found in the multiwavelength light curves (Xie *et al.* 2008; Abdo *et al.* 2010; Fu *et al.* 2014; Sandrinelli *et al.* 2016b).

In this paper, we performed two types of time-series analysis, namely, weighted wavelet Z-transform (WWZ; Foster 1996) and Lomb–Scargle periodogram (LSP; Lomb 1976; Scargle 1982) to the radio light curves of PKS 1510-089 for searching the possible long-term periodicities. In Section 2, we describe the observations of this source. We then present the QPO analysis of the light curves and the statistical significance of the detected periodicities in Section 3. Finally, we summarize our conclusions in Section 4.

2. Observations

The historical 4.8, 8, and 14.5 GHz radio observations of PKS 1510-089 were obtained from UMRAO located in Dexter, MI, USA. The UMRAO program employed rotating, dual-horn polarimeter feed systems to measure the total flux density and linear polarization until mid-2012. More details about the UMRAO program and data reduction can be found in Aller *et al.* (1985, 1999).

Table 1 summarizes the UMRAO observations including number of the data, time span, flux range, average flux, and fractional variability amplitude F_{var} (Edelson *et al.* 2002). It is feasible to detect potential periodicities from the light curves, of which the flux densities variability amplitudes F_{var} s increasing toward higher temporal frequencies are at rather strong values of 31–41% indicate moderate variabilities over the potential periodicities. The long-term light curves of PKS 1510-089 at 4.8, 8, and 14.5 GHz

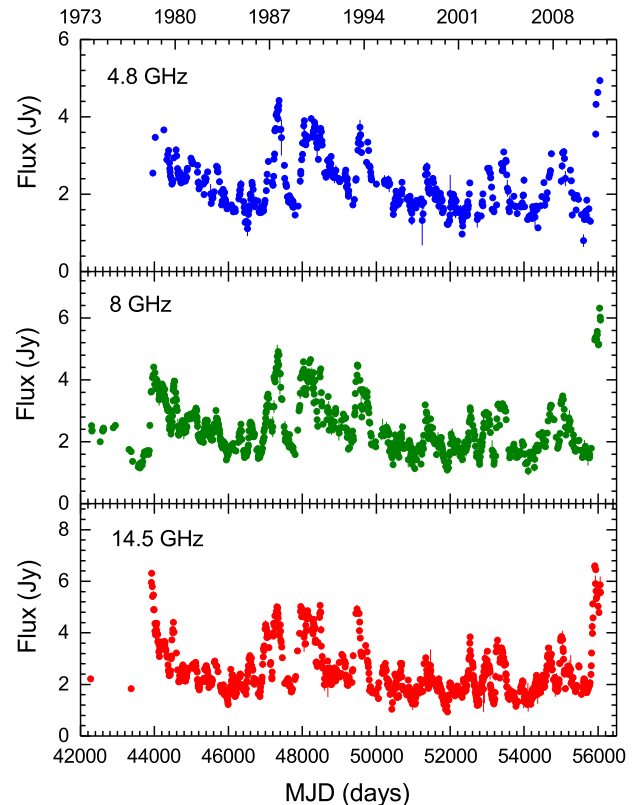


Figure 1. Weekly binned radio light curve of PKS 1510-089 from UMRAO spanning nearly 40 years. Panels (a), (b) and (c) show observations at 4.8, 8, and 14.5 GHz, respectively. Outliers in panel (c) (the first two data points) had been excluded in WWZ and LSP analyses.

with average sampling of a week are presented in Figure 1. On a visual inspection, it can be seen that the light curves at different radio frequencies present generally consistent features and that the intervals between many flares make the search for potential quasi-periodic flux modulations worthwhile.

3. Analysis and results

3.1 Weighted wavelet Z-transform

To identify and quantify any possible QPO, a modified wavelet analysis known as the WWZ was performed to the radio observations. The WWZ method has been

widely used to search for QPOs of blazars (An *et al.* 2013; King *et al.* 2013; Bhatta 2017, 2018; Zhang *et al.* 2018; Gupta *et al.* 2019; Kushwaha *et al.* 2020; Sarkar *et al.* 2020 and references therein). WWZ projects the wavelet transforms onto three trial functions: $\phi_1(t) = 1(t)$, $\phi_2(t) = \cos[\omega(t - \tau)]$ and $\phi_3(t) = \sin[\omega(t - \tau)]$, and also included statistical weights $\omega_\alpha = \exp(-c\omega^2(t_\alpha - \tau)^2)$ ($\alpha = 1, 2, 3$) on the projection, where c is a tunable parameter. The WWZ power estimates the significance of a detected periodicity with frequency ω and time shift τ in a statistical manner, i.e.,

$$\text{WWZ} = \frac{(N_{\text{eff}} - 3)V_y}{2(V_x - V_y)}, \quad (1)$$

where N_{eff} is the effective number of data points contributing to the signal, and V_x and V_y are the weighted variations of the uneven data x and the model function y , respectively. These factors are defined as follows:

$$N_{\text{eff}} = \frac{(\sum \omega_\alpha)^2}{\sum \omega_\alpha^2} = \frac{[\sum e^{-c\omega^2(t_\alpha - \tau)^2}]^2}{\sum e^{-2c\omega^2(t_\alpha - \tau)^2}},$$

$$V_x = \frac{\sum \omega_\alpha \omega_\alpha x^2(t_\alpha)}{\sum \omega_\alpha} - \left[\frac{\sum \omega_\alpha \omega_\alpha x(t_\alpha)}{\sum \omega_\alpha} \right]^2 = \langle x|x \rangle - \langle 1|x \rangle^2,$$

$$V_y = \frac{\sum \omega_\alpha \omega_\alpha y^2(t_\alpha)}{\sum \omega_\alpha} - \left[\frac{\sum \omega_\alpha \omega_\alpha y(t_\alpha)}{\sum \omega_\alpha} \right]^2 = \langle y|y \rangle - \langle 1|y \rangle^2. \quad (2)$$

In the denominators of V_x and V_y , parameters λ corresponds to the number of test frequencies.

The statistical behavior of the WWZ is suitable for determining the periodic fluctuation from irregularly sampled time series. Then, WWZ decomposes the data into observing epoch and frequency/time domain (WWZ map), in which the WWZ power peaks can be used to determine periodic components, check continuities of candidate periodicities, and track evolutions of periodicities or amplitudes. In practice, time-averaged WWZ power considering the strength of the signal at each frequency is also a useful approach for periodic fluctuation detection and significance estimation.

3.2 Periodicity search

As shown in Figure 2, the left-hand panel shows a color-scaled WWZ power for the 4.8 GHz light curve as a function of both time and period (frequency). In our WWZ analysis, the frequency range of 0.00025–0.01 day⁻¹, a period step of 10 day and a decay constant $c = 0.001$ were adopted. These parameters can properly strike a balance between frequency and time resolution. Moreover, for the range of 0.00025–0.01 day⁻¹, sufficient cycles in the light curves and the sampling feature of the data are taken into consideration. From the WWZ power plane, we observe quasi-periodic signals with dominant periods centered around 1050 and 1300 days primarily modulated in

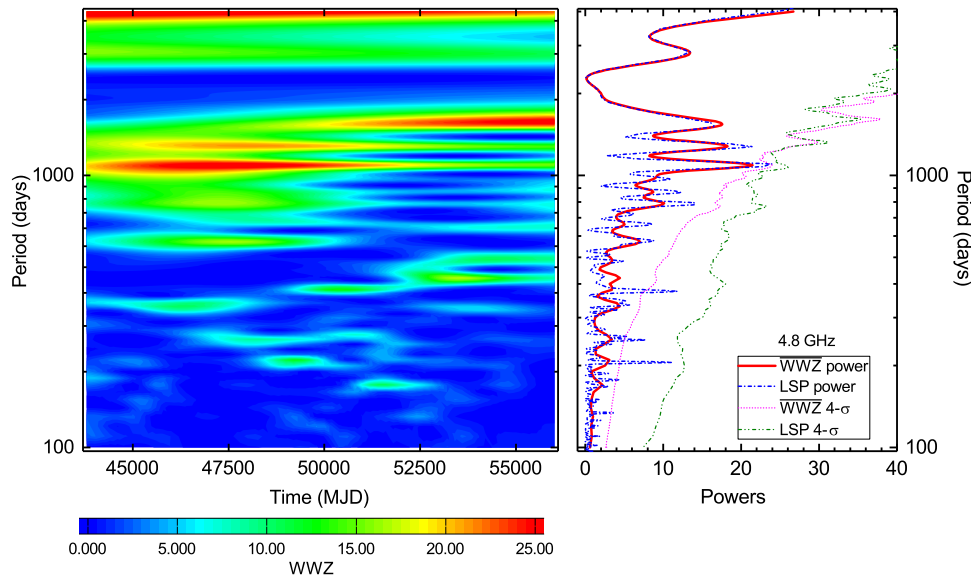


Figure 2. WWZ and LSP analysis of PKS 1510-089 for a 4.8 GHz radio light curve. The left-hand panel: the color-scaled WWZ power in the time-period plane. The right-hand panel: time-averaged WWZ power (red solid line) and the LSP power (blue dash-dotted line). The magenta dotted and olive dash double dotted curves in the right-hand panel correspond to 4 σ significance curves for WWZ and LSP analysis, respectively, obtained from the light curve simulation.

the first half of the observations while periodicity of ~ 1600 days mainly modulated in the last half of the observations. Moreover, other possible periodicities of ~ 580 , ~ 420 , ~ 375 , and ~ 200 days with lower WWZ power were supposed to be short term, not continuous.

The time-averaged WWZ power as a function of the period is shown in the right-hand panel of Figure 2, in which several WWZ power peaks stand out, generally consistent with the periodicities mentioned above, and the time-averaged WWZ power at a period of about 1000 days becomes the most pronounced quasi-periodic signal.

We then performed the LSP method on the weekly 4.8 GHz light curve for comparison, with the same temporal resolution as the WWZ analysis. The LSP is one of the basic and most widely used methods for periodicity analysis in non-uniformly sampled data. In the right panel of Figure 2, the normalized power of the LSP depicted by a blue dash-dotted line shows a good agreement with the time-averaged-WWZ power at low frequencies, while LSP power at ~ 375 , ~ 250 , and ~ 206 days becomes noticeably stronger at higher frequencies, indicating possible quasi-periodic signals.

With the same procedures and parameters, variations at 8 and 14.5 GHz have been analyzed by the WWZ and LSP methods, and the results are shown in Figures 3 and 4, respectively. In the left panel of Figure 3, quasi-periodic signals with periods centered around 1070, 800, and 570 days were observed, which have been confirmed by the time-averaged-WWZ power and LSP power. As shown in the left panel of

Figure 4, the WWZ power of the 14.5 GHz light curve shows a little difference from the WWZ powers of the 4.8 and 8 GHz light curve, i.e., a quasi-periodic signal of 430 days becomes more significant and mainly oscillates in the time range of modified Julian date (MJD) 51,000–MJD 55,000. Besides, the WWZ power, time-averaged-WWZ power and LSP power reveal quasi-periodic signals with periods centered around 1080, 860, and 570 days, indicating an accordant result again.

3.3 Significance estimation

In addition to the complicated and multiple features of the QPOs discussed above, LSP powers typically display larger amplitudes than the time-averaged-WWZ powers at high frequencies, as shown in Figures 1–3. Thus, it is necessary to assess the significance of these QPOs. At lower frequencies, the flux variability of blazars generally exhibits red noise behavior such that the periodograms can easily give rise to spurious periodicities (Press 1978; Vaughan 2005; Vaughan *et al.* 2016; Bhatta 2017; Li *et al.* 2017, 2018 and references therein). The red noise-dominated component can be fitted with a power-law model $P(f) \propto f^{-\alpha}$, where $P(f)$ is the power at temporal frequency f with spectral slope α .

We then determine the significance against the red noise spectrum of the observed light curve, following the procedure from Vaughan (2005). The red noise background was established by performing a large

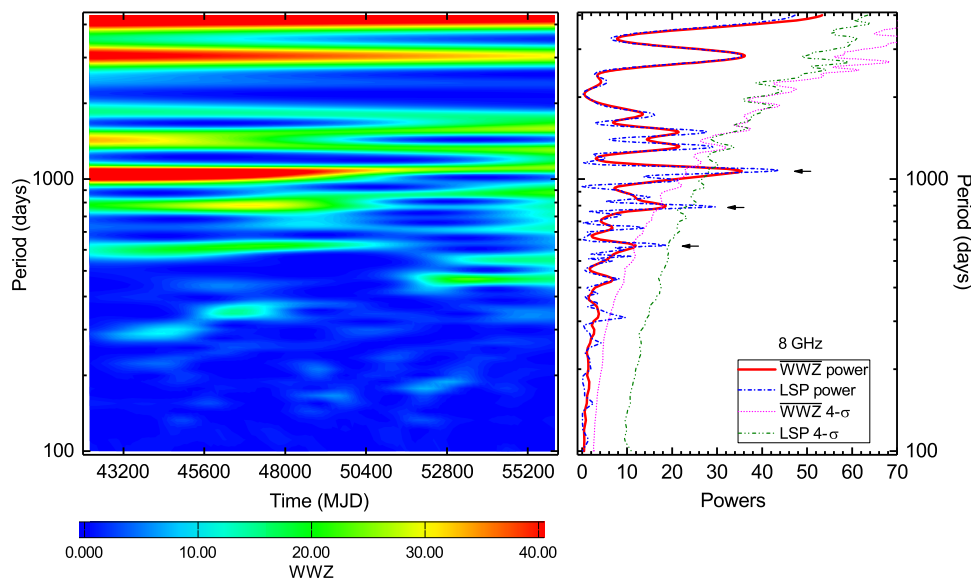


Figure 3. As in Figure 2 for the WWZ and LSP analysis of PKS 1510-089 for the 8 GHz light curve.

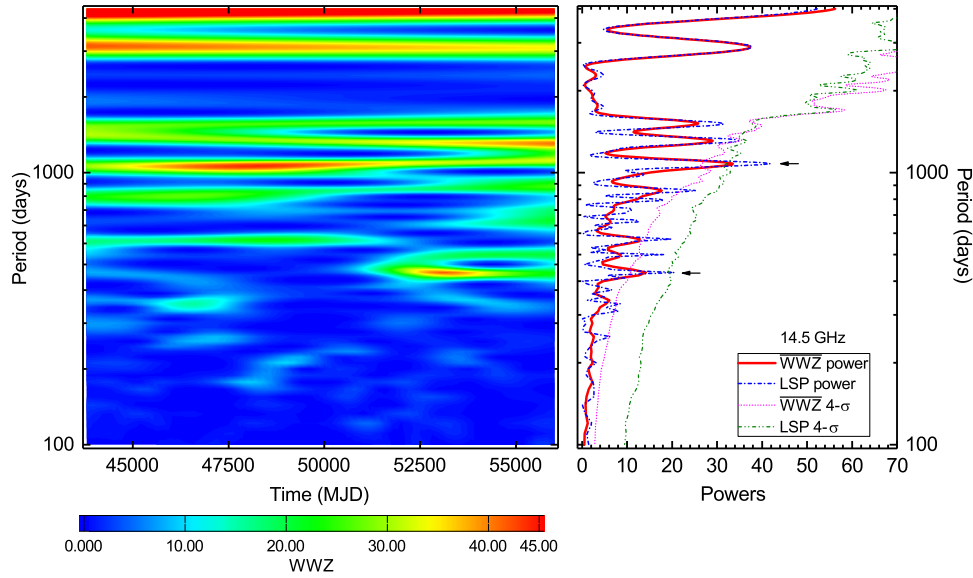


Figure 4. As in Figure 2 for the WWZ and LSP analysis of PKS 1510-089 for the 14.5 GHz light curve.

number of Monte Carlo simulations of the light curves obtained by randomizing the amplitude and the phase of the Fourier components (Timmer & Koenig 1995). For each waveband, 10,000 light curves were simulated assuming red noise with the same mean, standard deviation, sampling number, temporal baselines, and sampling interval as the original weekly binned light curve. To estimate the red noise continuum, spectral slopes $\alpha_{4.8\text{GHz}} = 0.90$, $\alpha_{8\text{GHz}} = 0.85$, and $\alpha_{14.5\text{GHz}} = 0.88$, were measured by fitting LSP periodograms with a power-law model. These power spectral slopes were estimated by fitting a linear function to the log-periodogram using the LSP method.

Then, these simulated light curves were used to establish the red noise backgrounds using the same procedures and parameters as the observed light curve in Section 3.2. In the right panels of Figures 1–3, 4σ confidence levels derived from the distributions of time-averaged-WWZ powers and LSP powers of the simulated light curves are shown as magenta dotted and olive dash double dotted curves, respectively. Overall, in each figure, the estimation of significance for time-averaged-WWZ powers and LSP powers shows no obvious discrepancy despite the differences between the WWZ and LSP confidence level curves, and possible QPOs with significance $>4\sigma$ are denoted by black arrows. Particularly, we determined no QPOs over the 4σ level in both WWZ and LSP analyses, for the significance estimation of the 4.8 GHz light curve (right panel in Figure 2). In Figure 3, QPOs with high WWZ powers and LSP powers at 1070, 800, and 570 days derived in Section 3.2 are detected above the corresponding WWZ and LSP 4σ confidence level,

indicating that there are at least three QPO components that can be confirmed in the 8 GHz light curve, at a high significance. However, the significance estimation of the 14.5 GHz light curve (right panel in Figure 4) represents some differences, i.e., the significances of the QPOs of 1080 and 430 days reach 4σ level in both WWZ and LSP analyses, while prominent QPOs of 800 and 570 days with significance $>4\sigma$ (right panel of Figure 3) that do not hit that level.

4. Discussion and conclusions

The UMRAO radio light curves of PKS 1510-089 spanning nearly 40 years have been weekly binned and cautiously analyzed by using the WWZ and LSP methods. Both analyses consistently revealed an accordant conclusion. To account for the red-noise processes, a large number of Monte Carlo simulations assuming a power-law model for the LSP and WWZ periodograms were performed to estimate the significance of these QPOs, and the results indicated that prominent QPOs of 570 ± 30 , 800 ± 30 , and 1070 ± 40 days stand out above the 4σ confidence interval in the 8 GHz light curve, 430 ± 10 and 1080 ± 30 days in the 14.5 GHz light curve, no QPOs in the 4.8 GHz light curve, respectively. Here, the uncertainties of the possible periodicities are evaluated on the basis of the half-width at half maximum of the Gaussian fitting centered at the maximum WWZ power. In our analysis, if we only consider QPOs with high significance ($>4\sigma$), there is no obvious harmonic and multiple relationships that can be found.

Although the most prominent QPO of about 1070 days with significance $>4\sigma$ at 8 and 14.5 GHz did not exactly persist the whole observations, it was also the strongest signal at 4.8 GHz and lasted the longest duration at high significance in the WWZ plots for all three frequencies, indicating that QPOs in blazars are complicated and transient.

Although the physical mechanism in blazars on long-term timescales is still an outstanding issue, a number of possible explanations, such as supermassive binary black hole (SMBBH) systems (Ackermann *et al.* 2015; Graham *et al.* 2015; Sandrinelli *et al.* 2016a,b), Lense–Thirring precession of accretion disks (Stella & Vietri 1998; Liska *et al.* 2018; Tavani *et al.* 2018), jet precession (Rieger 2004; Liska *et al.* 2018), helical structures in jets and perturbation processes (Villata & Raiteri 1999) have been proposed to explain the long-term periodic variability. We also note that PKS 1510-089 might be a good SMBBH candidate (Xie *et al.* 2008; Fu *et al.* 2014). Using the 37 and 22 GHz observations taken from the Metsähovi Radio Observatory, Xie *et al.* (2008) found two periods of 0.92 ± 0.04 and 1.82 ± 0.12 years consistent with the quasi-periodic flux minimum of 0.92 ± 0.03 year (Xie *et al.* 2002) and deep flux minima of 1.84 ± 0.1 year (Xie *et al.* 2004) in the optical band, and suggested an SMBBH system to explain the two periodic phenomena, i.e., the secondary black hole could penetrate twice the accretion disk of the primary black hole per one orbital period. Unfortunately, there are no QPOs of about 0.92 or 1.82 years that can be identified from both the WWZ and LSP analyses, even though the 3σ threshold is adopted.

Based on the UMRAO data at 4.8, 8, and 14.5 GHz of PKS 1510-089, a possible period of about 12 years was found by Fan *et al.* (2007). However, this possible period is obviously overestimated considering the time coverage of about 25 years and the lack of red noise background analysis. Recently, similarly to our work, Tripathi *et al.* (2021) analyzed the UMRAO radio light curves of AO 0235 + 164 at 4.8, 8, and 14.5 GHz by means of the data compensated discrete Fourier transform, LSP, and WWZ methods, and reported comparably strong QPO signals. It can be noted that their claimed QPOs against red noise background persist sufficient cycles, which are statistically meaningful. Therefore, we conclude that early QPO claims for blazar light curves without evaluating the statistical significance and/or accounting for the influences of the colored noise need to be reevaluated.

Acknowledgements

This research was supported by the National Natural Science Foundation of China (11903028), the Fundamental Research Plan of Yunnan Province, China (2017FD147), and the Science Research Project of Zhaotong University, China (2018xj04). We are very grateful to Dr Margo Aller for providing the UMRAO data. This research has made use of data from the University of Michigan Radio Astronomy Observatory, which was supported by the University of Michigan and by a series of Grants from the National Science Foundation, most recently AST-0607523, and NASA Fermi Grant Nos NNX09AU16G, NNX10AP16G, and NNX11AO13G.

References

- Abdo A. A., Ackermann M., Agudo I. *et al.* 2010, *Astrophys. J.*, 721, 1425
- Ackermann M., Ajello M., Albert A. *et al.* 2015, *Astrophys. J.*, 813, L41
- Ahnen M. L., Ansoldi S., Antonelli L. A. *et al.* 2017, *Astron. Astrophys.*, 603, A29
- Aleksić J., Ansoldi S., Antonelli L. A. *et al.* 2014, *Astron. Astrophys.*, 569, A46
- Aller H. D., Aller M. F., Latimer G. E. *et al.* 1985, *Astrophys. J. Suppl.*, 59, 513
- Aller M. F., Aller H. D., Hughes P. A. *et al.* 1999, *Astrophys. J.*, 512, 601
- An T., Baan W. A., Wang J.-Y. *et al.* 2013, *Mon. Not. Roy. Astron. Soc.*, 434, 3487
- Beaklini P. P. B., Dominici T. P., Abraham Z. 2017, *Astron. Astrophys.*, 606, A87
- Bhatta G., 2017, *Astrophys. J.*, 847, 7
- Bhatta G. 2018, *Galaxies*, 6, 136
- Bhatta, G. 2019, *Mon. Not. Roy. Astron. Soc.*, 487, 3990
- Castignani G., Pian E., Belloni T. M. *et al.* 2017, *Astron. Astrophys.*, 601, A30
- Edelson R., Turner T. J., Pounds K. *et al.* 2002, *Astrophys. J.*, 568, 610
- Fan J. H., Liu Y., Yuan Y. H. *et al.* 2007, *Astron. Astrophys.*, 462, 547
- Foster G. 1996, *Astrophys. J.*, 112, 170
- Fu J.-P., Zhang H.-J., Zhang X. *et al.* 2014, *Chin. Astron. Astrophys.*, 38, 367
- Graham M. J., Djorgovski S. G., Stern D. *et al.* 2015, *Nature*, 518, 74
- Gupta A. C., Srivastava A. K., Wiita P. J. 2018, *Astron. Astrophys.*, 616, L6
- Gupta A. C., Tripathi A., Wiita P. J. *et al.* 2019, *Mon. Not. Roy. Astron. Soc.*, 484, 5785
- King O. G., Hovatta T., Max-Moerbeck W. *et al.* 2013, *Mon. Not. Roy. Astron. Soc.*, 436, L114

- Kushwaha P., Sarkar A., Gupta A. C. *et al.* 2020, *Mon. Not. Roy. Astron. Soc.*, 499, 653
- Li X.-P., Luo Y.-H., Yang H.-Y. *et al.* 2017, *Astrophys. J.*, 847, 8
- Li X.-P., Luo Y.-H., Yang H.-Y. *et al.* 2018, *Astrophys. Space Sci.*, 363, 169
- Liska M., Hesp C., Tchekhovskoy A. *et al.* 2018, *Mon. Not. Roy. Astron. Soc.*, 474L, 81
- Liu B., Liu X. 2014, *Astrophys. Space Sci.*, 352, 215
- Lomb N. R., 1976, *Astrophys. Space Sci.*, 39, 447
- Mohan P., An T., Frey S. *et al.* 2016, *Mon. Not. Roy. Astron. Soc.*, 463, 1812
- Park J., Lee S.-S., Kim J.-Y. *et al.* 2019, *Astrophys. J.*, 877, 106
- Press W. H. 1978, *Comments Astrophysics*, 7, 103
- Raiteri C. M., Villata M., Aller H. D. *et al.* 2001, *Astron. Astrophys.*, 377, 396
- Rieger F. M. 2004, *Astrophys. J.*, 615, L5
- Sandrinelli A., Covino S., Treves A. 2016a, *Astrophys. J.*, 820, 20
- Sandrinelli A., Covino S., Dotti M. *et al.* 2016b, *Astrophys. J.*, 151, 54
- Sarkar A., Kushwaha P., Gupta A. C. *et al.* 2020, *Astron. Astrophys.*, 642, A129
- Scargle J. D. 1982, *Astrophys. J.*, 263, 835
- Stella L., Vietri M. 1998, *Astrophys. J.*, 492, L59
- Tavani M., Cavaliere A., Pere M.-A. *et al.* 2018, *Astrophys. J.*, 854, 11
- Thompson D. J., Djorgovski S., de Carvalho R. 1990, *Publ. Astron. Soc. Pac.*, 102, 1235
- Timmer J., Koenig M. 1995, *Astron. Astrophys.*, 300, 707
- Tripathi A., Gupta A. C., Aller M. F. *et al.* 2021, *Mon. Not. Roy. Astron. Soc.*, 501, 5997
- Vaughan S., Edelson R., Warwick R. S. *et al.* 2003, *Mon. Not. Roy. Astron. Soc.*, 345, 1271
- Vaughan S. 2005, *Astron. Astrophys.*, 431, 391
- Vaughan S., Uttley P., Markowitz A. G. *et al.* 2016, *Mon. Not. Roy. Astron. Soc.*, 461, 3145
- Villata M., Raiteri C. M. 1999, *Astron. Astrophys.*, 347, 30
- Wang J.-Y., An T., Baan W. A. *et al.* 2014, *Mon. Not. Roy. Astron. Soc.*, 443, 58
- Xie G. Z., Liang E. W., Zhou S. B. *et al.* 2002, *Mon. Not. Roy. Astron. Soc.*, 334, 459
- Xie G. Z., Zhou S. B., Li K. H. *et al.* 2004, *Mon. Not. Roy. Astron. Soc.*, 348, 831
- Xie G. Z., Yi T. F., Li H. Z. *et al.* 2008, *Astrophys. J.*, 135, 2212
- Zhang P.-f., Zhang P., Liao N.-h. *et al.* 2018, *Astrophys. J.*, 853, 193
- Zhou J., Wang Z., Chen L. *et al.* 2018, *Nature Commun.*, 9, 4599